Journal of Disability Research

2024 | Volume 3 | Pages: 1–8 | e-location ID: e20240002
DOI: 10.57197/JDR-2024-0002

Data Analysis of Biomechanical Dynamic Modeling of a Prosthetic Running Blade

Md Irfanul Haque Siddiqui[1,2,*], Nawaf Alamro[1,2,*] and Khalid Alluhydan[1,2,*]

[1]Mechanical Engineering Department, College of Engineering, King Saud University, Riyadh 11451, Saudi Arabia
[2]The King Salman Center for Disability Research, Riyadh, Saudi Arabia

Correspondence to:
Md Irfanul Haque Siddiqui*, e-mail: msiddiqui2.c@ksu.edu.sa
Nawaf Alamro*, e-mail: 441101243@student.ksu.edu.sa
Khalid Alluhydan*, e-mail: kalluhydan@ksu.edu.sa

Received: November 19 2023; Revised: January 2 2024; Accepted: January 2 2024; Published Online: January 31 2024

ABSTRACT

This study presents a comprehensive data analysis of the biomechanical performance of prosthetic running blades, utilizing vast data obtained from finite element simulations to elucidate the dynamics of force and energy under operational conditions. The primary focus is on understanding the behavior of these prosthetics at a speed of '1 *m/s*' and exploring the stability and fluctuations of various force and energy components. Key findings reveal that the kinetic energy of the blade and the total system energy exhibit minimal fluctuations, indicating a stable system behavior under the tested conditions. The normal contact force F_c shows a significant dynamic response, while the normal velocity V_y maintains a consistent downward trajectory, and the tangential force F_x remains essentially constant. Notably, a strong positive correlation between the force components F_c and F_x is observed, suggesting a synchronous relationship in their magnitudes. Additionally, a moderate negative correlation between the normal velocity V_y and the kinetic energies of the blade and system is identified, highlighting intricate interdependencies. This research contributes significantly to the understanding of prosthetic running blades, offering insights crucial for their design and optimization. The correlations and patterns identified underscore the need for further investigation into the causal relationships and practical implications of these dynamics in prosthetic technology.

KEYWORDS

biomechanical performance, finite element simulation, prosthetic design, prosthesis, biomechanics, running blade

INTRODUCTION

Biomechanics has long been integral to developing and refining prosthetic devices, focusing on the dynamic interactions between the human body and prosthetic components (Savin et al., 2023; Yaneva et al., 2023). In prosthetic running blades, explicit dynamic modeling emerges as a pivotal tool, enabling a deeper understanding of the complex biomechanical interactions. This approach is particularly relevant in the context of high-impact activities such as running, where the prosthetic must not only replicate but also enhance the natural movement of the human body (Al-Fareh et al., 2023; Dardari et al., 2023; Mohd Mukhtar et al., 2023; Murawa et al., 2023; Seratiuk Flores et al., 2023; Sidhu et al., 2023). The explicit dynamic modeling of a prosthetic running blade involves simulating the real-time physical behaviors of the blade under various conditions, such as different speeds, angles of impact, and forces. This type of analysis is crucial for understanding how the blade will perform under the rapid and high-stress conditions experienced during running (Bellmann et al., 2012; Zhang et al., 2019; Ahmed et al., 2023; Coltelli et al., 2023). It allows for examining stress distribution, strain patterns, and energy absorption and release, which are vital for optimizing the blade's design for performance and safety. One of the primary advantages of explicit dynamic modeling in biomechanics is its ability to handle complex material behaviors, including nonlinear elasticity, damping, and energy dissipation characteristics of prosthetic materials. This is particularly important for running blades, often made from advanced composite materials designed to store and release energy efficiently (Alluhydan et al., 2023). By accurately simulating these materials, researchers and engineers can predict how the blade will behave under different running conditions, leading to designs that maximize energy return and minimize the risk of injury to the user.

Furthermore, this approach allows for the exploration of various design parameters, such as the blade's shape, thickness, and curvature and their impact on the prosthetic's performance. This is crucial in a field where even minor adjustments can significantly affect an athlete's speed,

stability, and overall running mechanics. Modeling these parameters in a virtual environment significantly accelerates the design process, enabling rapid prototyping and testing without requiring extensive physical trials. Another critical aspect of this analysis is the interaction between the prosthetic blade and the ground. The explicit dynamic model can simulate various ground conditions, from the hardness of the track to the irregularities of the natural terrain. This provides invaluable insights into how changes in ground conditions affect the blade's performance, guiding the development of versatile designs that maintain optimal performance across different running environments.

Moreover, integrating explicit dynamic modeling with motion capture and other biomechanical analysis tools offers a comprehensive view of the prosthetic's performance. This integration allows for the correlation of simulation data with real-world biomechanical data, such as the forces exerted by the athlete's residual limb on the prosthetic socket. Such holistic analysis is essential for developing prosthetics that are not only high-performing but also comfortable and safe for long-term use. In conclusion, the explicit dynamic modeling of a prosthetic running blade represents a significant advancement in biomechanics. This approach plays a crucial role in developing next-generation prosthetics by providing detailed insights into the dynamic behavior of prosthetic blades under various conditions.

Numerical modeling facilitates a detailed assessment of the performance of the prosthetic running blade, encompassing elements like stress distribution, strain patterns, and energy absorption (Sancisi and Parenti-Castelli, 2011; Richard et al., 2016). Furthermore, numerical modeling aids in the optimization of design by examining different parameters, including materials, geometries, and structural configurations. Comprehending the static behavior of these blades is vital for their design and performance optimization (Groothuis and Houdijk, 2019; Yusof et al., 2021; Barnett et al., 2022). The blade must display favorable attributes like stiffness, flexibility, and energy storage capacity. Stiffness is a critical characteristic, dictating the extent of deformation or bending under load. A harmonious balance between stiffness and flexibility is essential to guarantee optimal energy return and efficient running mechanics. Zadpoor et al. (2007) conducted simulations on two distinct shoe types. Their parametric analysis aimed to explore the impact of various factors, such as mass, stiffness, damping, and gravity, on impact dynamics. The results revealed that impact forces escalated with increasing mass and touchdown velocities. Additionally, the study found that the effect of damping coefficients on impact force was more significant than that of stiffness.

Moreover, explicit dynamic analysis is a computational technique for simulating the dynamic response of prosthetic running blades under diverse loading conditions. This analytical method is essential for comprehending the blade's behavior during high-impact activities like running and jumping. By modeling the blade with realistic material properties, considering its nonlinear elasticity, damping, and energy dissipation characteristics, the simulation can more accurately depict the dynamic response of the blade. This approach provides a detailed understanding of the blade's performance across various loading scenarios (Bi et al., 2012). In the current study, finite element simulations were employed to analyze the biomechanical performance of the running blade. An explicit dynamic finite element analysis was carried out to study the blade's motion after an impact and quantify energy dissipation during the impact event. Furthermore, results have been discussed with the help of data analysis.

NUMERICAL MODELING

In this research, we used a carbon fiber epoxy composite material to simulate a prosthetic running blade (Siddiqui et al., 2023a,b,c). We devised a novel blade design, and meticulously studied and transformed it into a three-dimensional computer aided design (CAD) model using SpaceClaim software (Ansys Inc.). The design underwent meshing and structural analysis using Ansys Mechanical software. For our numerical investigation, a force of 1100 N was applied vertically atop the running blade assembly to analyze its static behavior. Our blade design draws inspiration from commercially available models, and the specific dimensions and meshing details are illustrated in Figure 1.

Furthermore, we conducted explicit finite element numerical modeling of the prosthetic running blades. The material and geometric properties are shown in Table 1, while the CAD diagram of the prosthetic running blade, complete

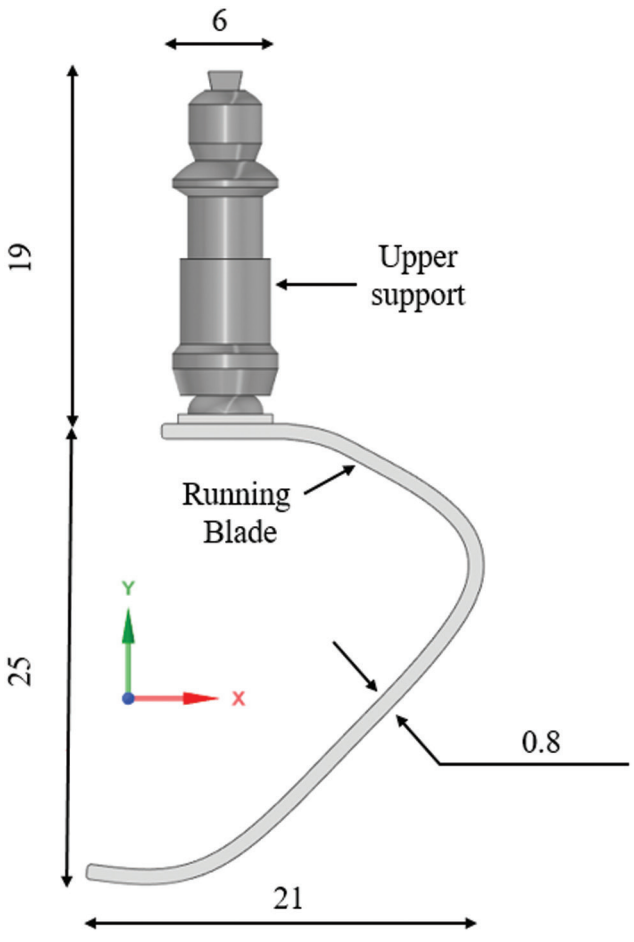

Figure 1: Dimensions of the prosthetic running blade.

Table 1: Material properties (Noroozi et al., 2013; Sundararaj and Subramaniyan, 2020; Ouarhim et al., 2021; Talla et al., 2021).

No	Property	Materials Carbon fiber
1	Modulus of elasticity (GPa)	230
2	Poisson's ratio	0.2
3	Yield strength (MPa)	2500
4	Tensile strength ultimate (MPa)	3590
5	Comp. strength (MPa)	–
6	Density (kg/m^3)	1750
7	Melting point (C)	3652

with all dimensions, is presented in an accompanying figure. The blade, constructed using carbon fiber known for its high restitution, was modeled with a specific number of elements determined through a grid independence test.

RESULTS AND DISCUSSION

Figure 2 corresponds to the '1 *m/s*' speed for a comprehensive understanding of the forces and energies involved. Initially observed, the normal contact force F_c commenced

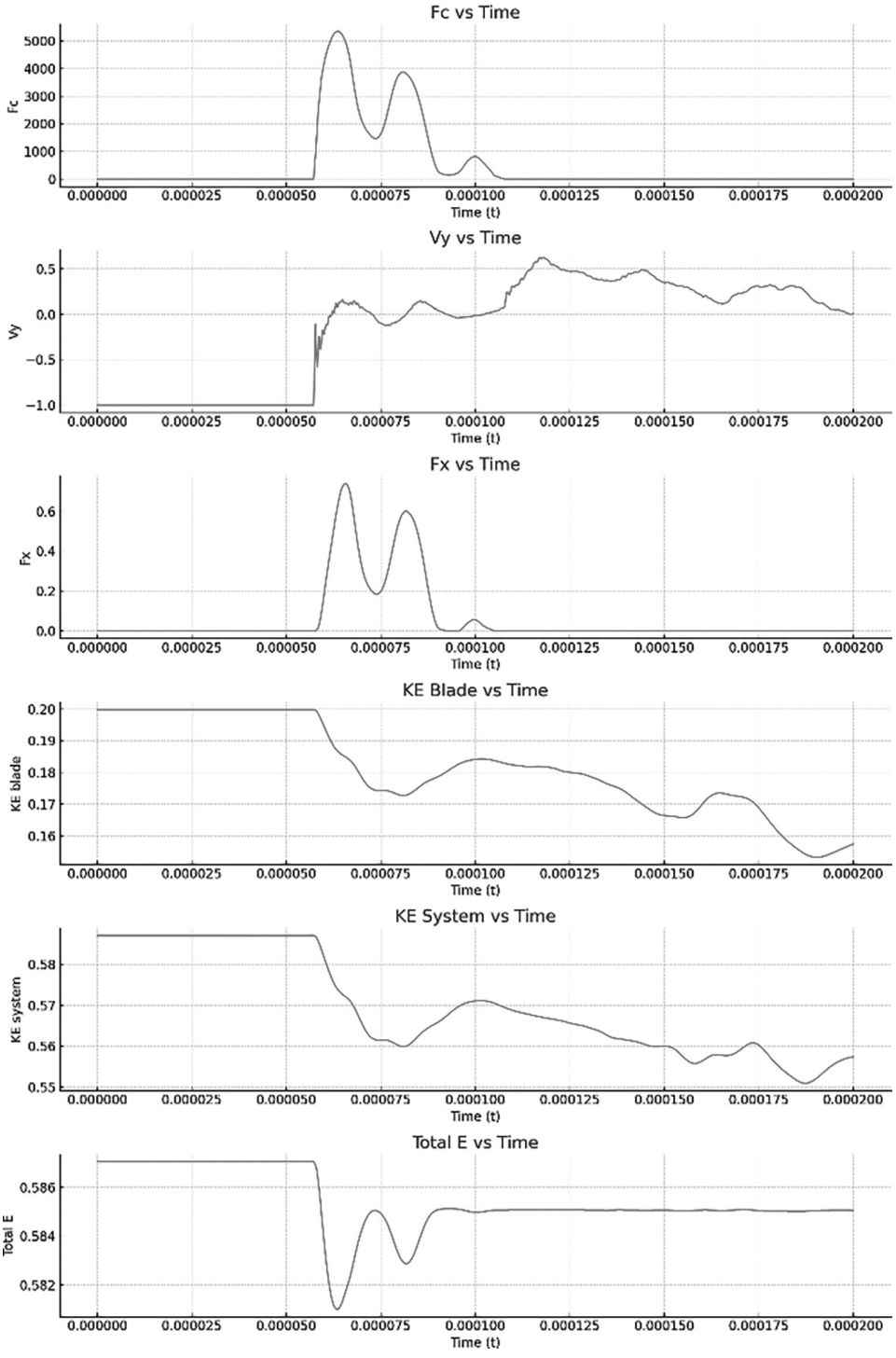

Figure 2: Forces, velocity, and energy plots. Abbreviation: KE, kinetic energy.

at a null value, undergoing some fluctuations before stabilizing. Conversely, the normal velocity V_y consistently maintained a steady, negative value, indicative of a continual downward trajectory. The tangential force F_x displayed no variation, remaining at 0 throughout the observation period. Regarding energy dynamics, both the blade's kinetic energy (*KE*) and the system's total *KE* were marked by their unchanging nature. Similarly, the total energy of the system remained constant. These findings collectively suggested that at a speed of '1 *m/s*,' the system was characterized by either stable values or minimal fluctuations. For the normal contact force F_c, the recorded values extended from a minimum of 0 to a peak of 5348.3 *N*. Notably, the median value was 0, indicating that the force was nonexistent for at least half of the observation period. The considerable disparity between the mean and median values suggested the presence of significant fluctuations or extreme values within this dataset. The normal velocity V_y varied from −1 *m/s* to around 0.63 *m/s*, with an average of about −0.14 *m/s*. This negative average, alongside a 25th percentile of −1 *m/s*, implied a predominantly negative velocity over a substantial portion of the time frame. The tangential force F_x displayed a relatively narrow range, from −0.0016 *N* to 0.7408 *N*, and with both mean and median values approximating 0, this indicated an almost constant 0 value throughout the observation. The *KE* of the blade denoted as *KE* blade, exhibited a limited range from 0.1533 *J* to 0.1998 *J*, with a mean around 0.1813 *J*, signifying a minimal variation. Similarly, the system's *KE* ranged from 0.5509 *J* to 0.5871 *J*, with an average of 0.5699 *J*. Lastly, the total energy, labeled Total *E*, had a very narrow range, from 0.581 *J* to 0.5871 *J*, maintaining remarkable consistency as evidenced by the small standard deviation. Finally, Figure 2 provides significant information during the contact process, which helps in understanding the dynamic effects of contact on the running blade.

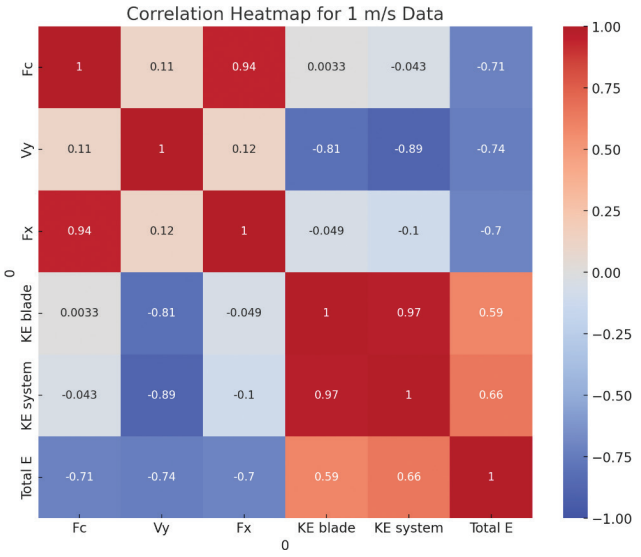

Figure 3: The boxplot for the kinematic, kinetic, and energetic components. Abbreviation: KE, kinetic energy.

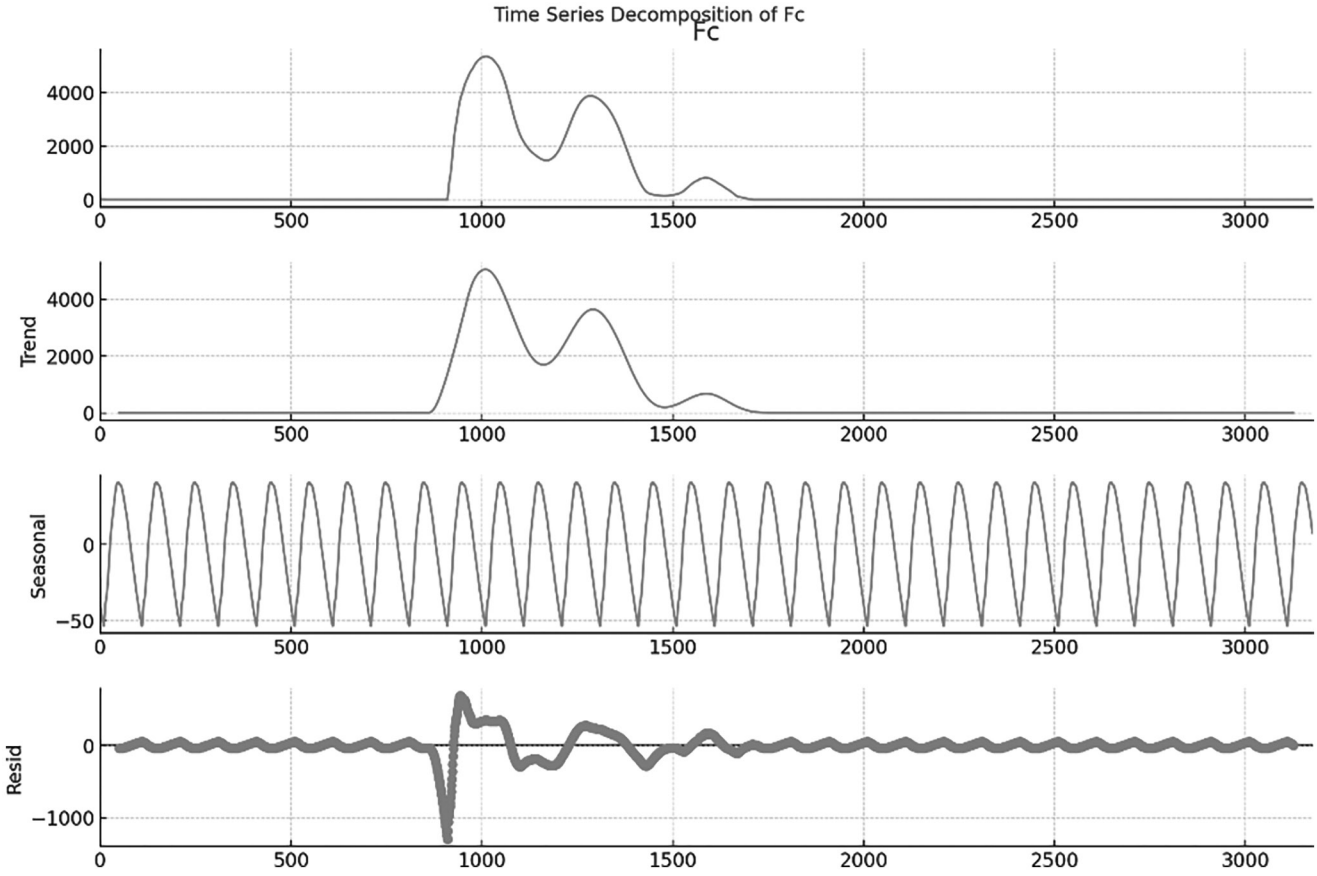

Figure 4: Time series analysis of the normal contact force F_c.

The heat map in Figure 3 is a visual representation of the interrelationships between different variables within the '1 *m/s*' data set. A notable finding was the strong positive correlation, approximately 0.92, between the force components F_c and F_x. This correlation suggested that an increase in the other typically mirrored an increase in one of these forces. Conversely, the normal velocity V_y and the *KE* of the blade, *KE* blade, exhibited a moderate negative correlation of around −0.47. This indicated that an increase in V_y generally coincided with a decrease in the blade's *KE*. A similar moderately negative correlation, approximately −0.52, was observed between V_y and *KE*, where an increase in V_y tended to result in a reduction in the system's *KE*. Other variable pairings demonstrated weak or negligible correlations, implying a lack of strong linear relationships between them. While these correlations provided insights into potential interactions between variables, it was critical to acknowledge that correlation does not imply causation. Therefore, further investigation or experimental studies would be necessary to determine causal connections, which will provide helpful information in the design and manufacturing processes. Finally, the heat map encapsulates and correlates all necessary kinematic, kinetic, and energetic properties.

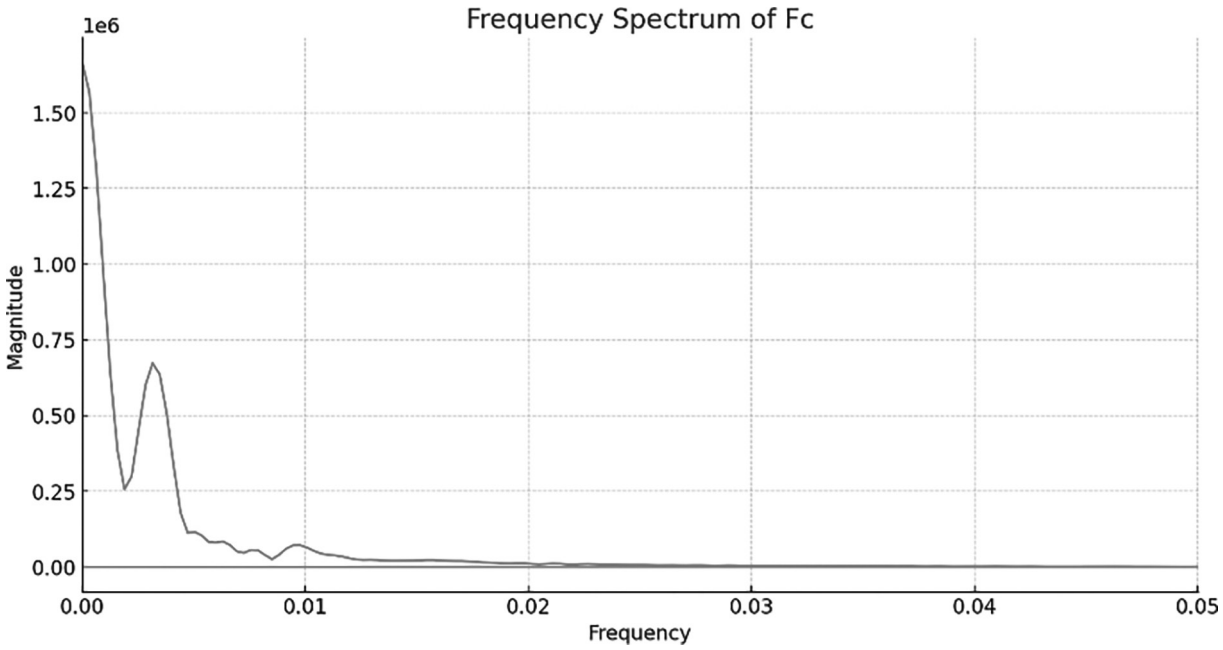

Figure 5: Normal contact force F_c and frequency plot.

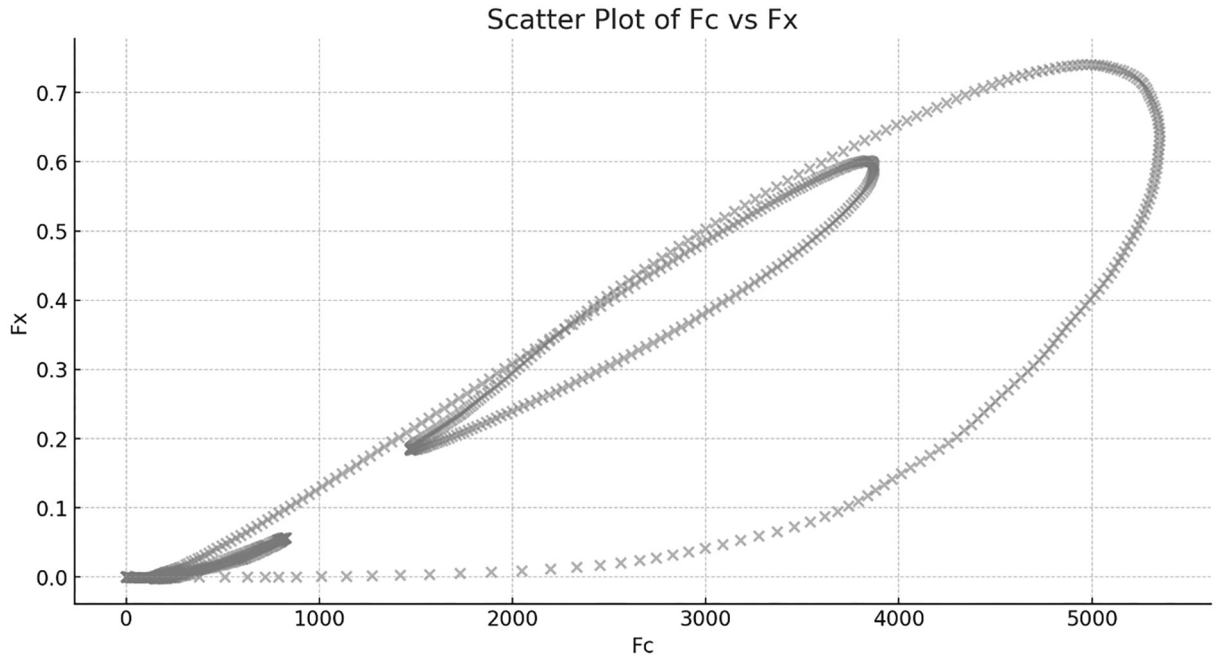

Figure 6: Phase plane of F_c and F_x.

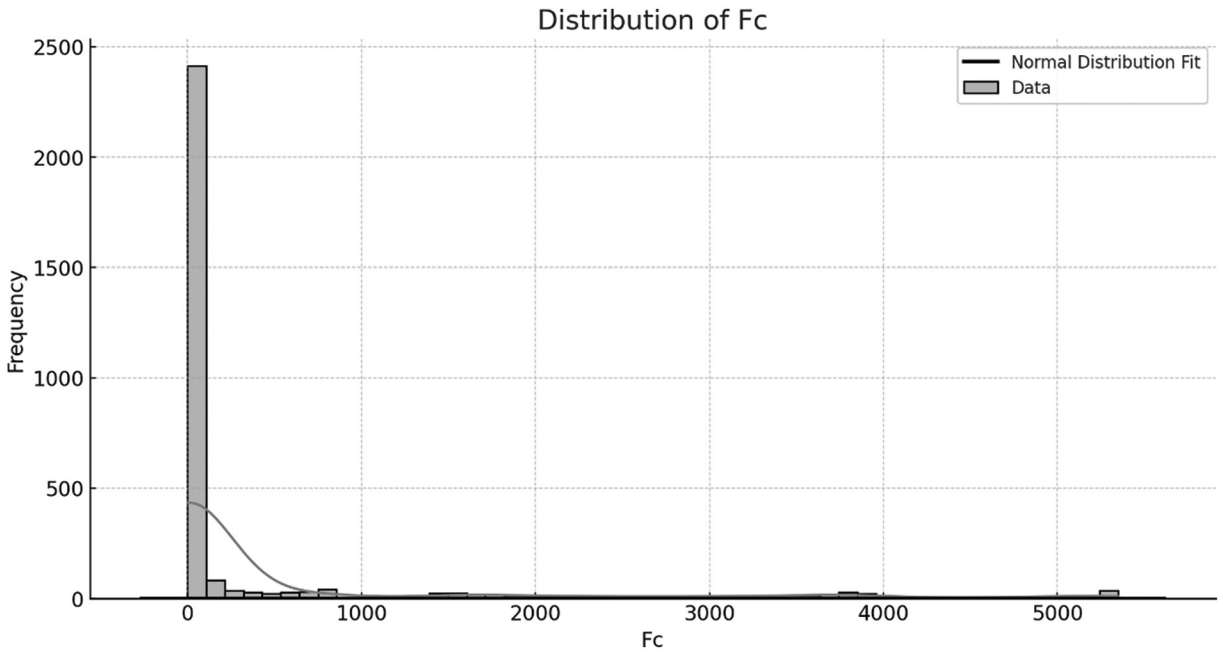

Figure 7: Frequency and contact force F_c plot.

Figure 4 shows the observed component of the actual time series data for the contact force F_c. The trend component of the data elucidated an underlying pattern, exhibiting some initial fluctuations before stabilizing and maintaining a relatively flat trajectory after the contact. The seasonal component highlighted the periodic nature of the data, with discernible repeating patterns becoming apparent. A periodicity of 100-time units was identified as a suitable fit, indicating a cyclical behavior recurring at this interval. Finally, the residual component that comprised the data remaining after both the trend and seasonal factors had been considered.

Figure 5 depicts the frequency spectrum of the contact force variable F_c. Positions closer to the origin represented lower frequencies, corresponding to long-term fluctuations, while those further from the origin denoted higher frequencies, indicative of short-term fluctuations. The emergence of peaks within this spectrum highlighted significant frequencies within the dataset. Upon observational analysis of the plot, several low-frequency peaks were identified. These peaks suggested the presence of periodic patterns or cycles within the F_c data. These observations emphasized the potential for underlying systematic behaviors or regularities in the temporal sequence of the force measurements. In addition, understanding the frequency response is helpful in analyzing the nonlinear dynamics of the prosthetic running blade's design, stability, and dynamic behavior.

The parametric plot in Figure 6 depicts the interdependence between the friction and contact force components F_c and F_x. It provides a significant understanding between normal and tangential components of the contact forces. A notable concentration of data points was observed clustering near the origin, indicating that the values for both F_c and F_x were frequently close to 0. Additionally, there was a discernible ascending trajectory of data points, suggesting that an increase in F_x was typically accompanied by an increase in F_c. This pattern aligned with these two variables previously identified strong positive correlation. The visualization thus provided empirical support for a synchronous relationship in the magnitudes of F_c and F_x.

The histogram provided a visual representation (as shown in Fig. 7) of the force variable F_c distribution characteristics. It featured a significant concentration of data points around the 0 value. Furthermore, the distribution was characterized by an elongated tail on the right side, signifying the presence of higher force values. These were consistent with the outliers previously identified in the data. Overlaying the histogram, a black line depicted the theoretical fit for a normal distribution. Upon comparison, it was evident that the actual distribution of F_c deviated from normalcy. Such a distributional shape, characterized by a concentrated peak followed by a protracted tail, is commonly observed in various empirical phenomena. Finally, comprehensive frequency analyses are effective in understanding dynamic stability, which provides meaningful information on the selection of materials and the design process.

CONCLUSIONS

The comprehensive analysis of prosthetic running blades, as presented in this study, offers significant insights into the biomechanical performance of these devices. The results, primarily derived from a series of detailed simulations and graphical representations, reveal intricate aspects of the forces and energies involved in the functioning of prosthetic blades. The study's findings indicate a stable force and energy variable behavior at a speed of '1 *m/s*', with minimal fluctuations observed in the blade's *KE* and the system's total energy. The normal contact force F_c displayed significant fluctuations, suggesting a dynamic response to varying conditions, while the normal velocity V_y maintained

a consistent negative trajectory, indicative of a continuous downward motion. The tangential force F_x remained constant, reinforcing the system's stability. A notable aspect of the study is the strong positive correlation identified between the force components F_c and F_x, suggesting a synchronous increase in these forces.

Conversely, a moderate negative correlation was observed between the normal velocity V_y and the kinetic energies of the blade and the system, indicating a decrease in *KE* with an increase in V_y. These correlations, while insightful, necessitate further investigation to establish causation. The time series analysis of F_c revealed a cyclical behavior with periodic fluctuations, highlighting the importance of considering temporal patterns in understanding the dynamics of prosthetic blades. The frequency spectrum analysis further emphasized the presence of significant low-frequency peaks, suggesting underlying systematic behaviors in the force measurements. The distribution characteristics of F_c, as depicted in the histogram, showed a pronounced peak at 0 with an elongated tail, indicating the occurrence of higher force values less frequently. This skewness and deviation from a normal distribution pattern underscore the complexity of the forces acting on prosthetic blades. This study provides a detailed understanding of the biomechanical behavior of prosthetic running blades, emphasizing the importance of considering various force and energy dynamics. In addition, it provides valuable insights for future design and optimization purposes. The correlations and patterns identified offer valuable insights for future design and optimization of these prosthetics. However, they also highlight the need for further research to fully comprehend the relationships and practical implications of these findings.

ACKNOWLEDGMENTS

The authors extend their appreciation to the King Salman Center for Disability Research for funding this work through Research Group no KSRG-2022-049.

CONFLICTS OF INTEREST

The authors declare no conflicts of interest in association with the present study.

REFERENCES

Ahmed M.H., Kutsuzawa K. and Hayashibe M. (2023). Transhumeral arm reaching motion prediction through deep reinforcement learning-based synthetic motion cloning. *Biomimetics*, 8(4), 367. 10.3390/BIOMIMETICS8040367.

Al-Fareh A., Dubais M., Smran A., El Bahra S. and Samran A. (2023). Awareness, knowledge, and perception of tooth-supported and implant-supported prostheses among adults in Sana'a city: a survey-based study. *Oral*, 3(3), 337-352. 10.3390/ORAL3030028.

Alluhydan K., Siddiqui M.I.H. and Elkanani H. (2023). Functionality and comfort design of lower-limb prosthetics: a review. *J. Disabil. Res.*, 2(3), 10-23. 10.57197/JDR-2023-0031.

Barnett C.T., De Asha A.R., Skervin T.K., Buckley J.G. and Foster R.J. (2022). Spring-mass behavioural adaptations to acute changes in prosthetic blade stiffness during submaximal running in unilateral transtibial prosthesis users. *Gait Posture*, 98, 153-159. 10.1016/j.gaitpost.2022.09.008.

Bellmann M, Schmalz T, Ludwigs E. and Blumentritt S. (2012). Immediate effects of a new microprocessor-controlled prosthetic knee joint: a comparative biomechanical evaluation. *Arch. Phys. Med. Rehabil.*, 93(3), 541-549. 10.1016/J.APMR.2011.10.017.

Bi S.S., Zhou X.D. and Marghitu D.B. (2012). Impact modelling and analysis of the compliant legged robots. *Proc. Inst. Mech. Eng. Pt. K J. Multi-body Dyn.*, 226(2), 85-94. 10.1177/1464419312441451.

Coltelli M.A., Keeven J.M., Leckie J.M., Catterlin J.K., Sadagic A. and Kartalov E.P. (2023). Output force density saturation in COMSOL simulations of biomimetic artificial muscles. *Appl. Sci.*, 13(16), 9286. 10.3390/APP13169286.

Dardari M., Cinteza E., Vasile C.M., Padovani P. and Vatasescu R. (2023). Infective endocarditis among pediatric patients with prosthetic valves and cardiac devices: a review and update of recent emerging diagnostic and management strategies. *J. Clin. Med.*, 12(15), 4941. 10.3390/JCM12154941.

Groothuis A. and Houdijk H. (2019). The effect of prosthetic alignment on prosthetic and total leg stiffness while running with simulated running-specific prostheses. *Front. Sports Act. Living*, 1, 16. 10.3389/fspor.2019.00016.

Mohd Mukhtar N.Q., Shuib S., Anuar M.A., Mohd Miswan M.F. and Mohd Anuar M.A. (2023). Design optimisation of bi-cruciate retaining total knee arthroplasty (TKA) prosthesis via Taguchi methods. *Mathematics*, 11(2), 312. 10.3390/MATH11020312.

Murawa M., Otworowski J., But S., Kabacinski J., Kubaszewski L. and Gramala A. (2023). Symmetry function in trans-tibial amputees gait supplied with the new concept of affordable dynamic foot prosthesis—case study. *Symmetry*, 15(8), 1595. 10.3390/SYM15081595.

Noroozi S., Sewell P., Rahman A.G.A., Vinney J., Chao O.Z. and Dyer B. (2013). Modal analysis of composite prosthetic energy-storing-and-returning feet: an initial investigation. *Proc. Inst. Mech. Eng. Pt. P J. Sports Eng. Tech.*, 227(1), 39-48. 10.1177/1754337112439274.

Ouarhim W., Ait-Dahi M., Bensalah M.O., El Achaby M., Rodrigue D., Bouhfid R., et al. (2021). Characterization and numerical simulation of laminated glass fiber–polyester composites for a prosthetic running blade. *J. Reinf. Plast. Compos.*, 40(3-4), 118-133. 10.1177/0731684420949662.

Richard V., Lamberto G., Lu T.W., Cappozzo A. and Dumas R. (2016). Knee kinematics estimation using multi-body optimisation embedding a knee joint stiffness matrix: a feasibility study. *PLoS One*, 11(6), e0157010. 10.1371/JOURNAL.PONE.0157010.

Sancisi N. and Parenti-Castelli V. (2011). A sequentially-defined stiffness model of the knee. *Mech. Mach. Theory*, 46(12), 1920-1928. 10.1016/j.mechmachtheory.2011.07.006.

Savin L., Pinteala T., Mihai D.N., Mihailescu D., Miu S.S., Sirbu M.T., et al. (2023). Updates on biomaterials used in total hip arthroplasty (THA). *Polymers*, 15(15), 3278. 10.3390/POLYM15153278.

Seratiuk Flores H., Yeoh W.L., Loh P.Y., Morinaga K. and Muraki S. (2023). Biomechanical analysis of recreational cycling with unilateral transtibial prostheses. *Prosthesis*, 5(3), 733-751. 10.3390/PROSTHESIS5030052.

Siddiqui M.I.H., Alnaser I.A. and Alluhydan K. (2023a). Assessment of a carbon fiber prosthetic running blade for enhanced reliability. *Eksploat. i Niezawodn. – Maintenance and Reliability*, 25(4), 172668. 10.17531/EIN/172668.

Siddiqui M.I.H., Arifudin L., Alnaser I.A. and Alluhydan K. (2023b). Numerical investigation on the performance of prosthetic running blades by using different materials. *J. Disabil. Res.*, 2(1), 6-13. 10.57197/JDR-2023-0001.

Siddiqui M.I.H., Arifudin L., Alnaser I.A., Hassan A. and Alluhydan K. (2023c). Static behavior of a prosthetic running blade made from alloys and carbon fiber. *J. Disabil. Res.*, 2(1), 63-74. 10.57197/JDR-2023-0010.

Sidhu S., Persad P.J., Lam B.L., Zann K.L. and Gregori N.Z. (2023). Current assistive devices usage and recommendations for a future artificial vision prosthesis among patients with severe visual impairment due to inherited retinal diseases. *J. Clin. Med.*, 12(16), 5283. 10.3390/JCM12165283.

Sundararaj S. and Subramaniyan G.V. (2020). Structural design and economic analysis of prosthetic leg for below and above knee amputation. *Mater. Today Proc.*, 37(Part 2), 3450-3460. 10.1016/j.matpr.2020.09.331.

Talla H.K., Oleiwi J.K. and Hassan A.K.F. (2021). Performance of athletic prosthetic feet made of various composite materials with pmma matrix: numerical and theoretical study. *Rev. des Compos. et des Mater. Av.*, 31(4), 257-264. 10.18280/rcma.310410.

Yaneva A., Shopova D., Bakova D., Mihaylova A., Kasnakova P., Hristozova M., et al. (2023). The progress in bioprinting and its potential impact on health-related quality of life. *Bioengineering (Basel)*, 10(8), 910. 10.3390/BIOENGINEERING10080910.

Yusof K.H., Zulkipli M.A., Ahmad A.S., Yusri M.F., Al-Zubaidi S. and Mohammed, M.N. (2021). Design and development of prosthetic leg with a mechanical system. In: *Proceedings of the 2021 IEEE 12th Control and System Graduate Research Colloquium (ICSGRC 2021)*, Shah Alam, Malaysia, 7 August 2021. 10.1109/ICSGRC53186.2021.9515198.

Zadpoor A.A., Asadi Nikooyan A. and Reza Arshi A. (2007). A model-based parametric study of impact force during running. *J. Biomech.*, 40(9), 2012-2021. 10.1016/j.jbiomech.2006.09.016.

Zhang T., Bai X., Liu F. and Fan Y. (2019). Effect of prosthetic alignment on gait and biomechanical loading in individuals with transfemoral amputation: a preliminary study. *Gait Posture*, 71, 219-226. 10.1016/j.gaitpost.2019.04.026.